

# Interaction of Monovalent Ions with Hydrophobic and Hydrophilic Colloids: Charge Inversion and Ionic Specificity

Carles Calero and Jordi Faraudo\*

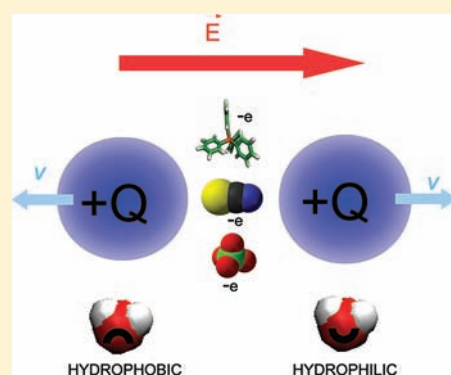
Institut de Ciència de Materials de Barcelona (ICMAB-CSIC), Campus de la UAB, 08193 Bellaterra, Spain

Delfi Bastos-González\*

Biocolloid and Fluid Physics Group, Department of Applied Physics, University of Granada, Avenida Fuentenueva S/N, 18071 Granada, Spain

**S** Supporting Information

**ABSTRACT:** Here we study experimentally and by simulations the interaction of monovalent organic and inorganic anions with hydrophobic and hydrophilic colloids. In the case of hydrophobic colloids, our experiments show that charge inversion is induced by chaotropic inorganic monovalent ions but it is not induced by kosmotropic inorganic anions. For organic anions, giant charge inversion is observed at very low electrolyte concentrations. In addition, charge inversion disappears for both organic and inorganic ions when turning to hydrophilic colloids. These results provide an experimental evidence for the hydrophobic effect as the driving force for both ion specific effects and charge inversion. In the case of organic anions, our molecular dynamics (MD) simulations with full atomic detail show explicitly how the large adsorption free energies found for hydrophobic colloids are transformed into large repulsive barriers for hydrophilic colloids. Simulations confirm that solvation free energy (and hence the hydrophobic effect) is responsible for the build up of a Stern layer of adsorbed ions and charge inversion in hydrophobic colloids and it is also the mechanism preventing charge inversion in hydrophilic colloids. Overall, our experimental and simulation results suggest that the interaction of monovalent ions with interfaces is dominated by solvation thermodynamics, that is, the chaotropic/kosmotropic character of ions and the hydrophobic/hydrophilic character of surfaces.



## I. INTRODUCTION

The interaction of interfaces with electrolytes is of key importance in determining physicochemical properties and functionality of systems as diverse as macromolecules, colloids, membranes, or microfluidic devices.<sup>1</sup> In spite of the substantial progress achieved in recent years in both experimental and theoretical methods (including all-atomic molecular dynamics simulations), several puzzling effects still lack a deep physical understanding. We recall here two particularly important cases, which have been found in a wide range of different soft matter systems and have received extensive experimental and theoretical attention. The first one is the question of the origin of ionic specificity. By ionic specificity, we mean that in a wide range of phenomena (surface tensions, colloidal stability, protein precipitation, etc.) one finds that ions with the same valency induce different behavior.<sup>2–4</sup> Quite surprisingly, these specific effects of ions can be ranged according to a series common to all the different observed phenomena, series which are known as Hofmeister series. Depending on its position on the series, the ions are traditionally called kosmotropic or chaotropic. These names arise from a hypothetical effect of the ions on water structure (creation or destruction), a point which is controversial.<sup>5</sup> Experimentally,

Hofmeister series correlate on the hydration behavior of ions.<sup>2,6</sup> Also, recent experiments show that these Hofmeister or ion specific effects depend crucially on the nature of the intervening interfaces.<sup>7,8</sup> They show that the position of particular ions within the series can be altered and even the whole series can be inverted by considering surfaces of different degree of hydrophobic/hydrophilic character. In fact, the mechanism underlying Hofmeister series is still controversial and it is attributed to different origins by different researchers. For example, the extensive work of Collins (summarized in his law of matching affinities) attributes these effects to pairing between ions and charged interfacial groups found at the surfaces of proteins (such as amine or carboxyl groups) with have similar (matching) solvation free energies.<sup>4,9</sup> In contrast, a recent theory predicts Hofmeister effects in surface tensions<sup>10,11</sup> and colloidal stability<sup>12</sup> based on the polarizability and size of ions. And yet another recent theoretical study<sup>13</sup> (based on molecular dynamics simulations) claims that cooperative, thermodynamic factors with no single,

Received: May 10, 2011

Published: August 08, 2011

direct microscopic origin are beyond the relative affinity of ions for interfaces.

The other, apparently unrelated open problem which we would like to address is charge inversion<sup>14–17</sup> (also known as overcharging or charge reversal). It refers to the attraction of counterions to an interface in excess of its own bare charge. Traditionally, charge inversion has been attributed to chemical binding between ions and surfaces.<sup>16</sup> However, the effect seems to be found almost exclusively in the case of multivalent ions and strongly charged interfaces (with few exceptions, see ref 18). Semiempirical models of ionic correlations near a strongly charged uniform surface<sup>14,15</sup> allow for charge inversion with multivalent ions without considering any chemical detail of the interface. Simulations of more realistic coarse-grained models<sup>19</sup> and also molecular dynamics simulations (including interfacial details and explicit water)<sup>17</sup> point to ionic correlations as a driving force for charge inversion. This concept is also supported by several works comparing theories, simulations, and experiments in systems such as latex colloids,<sup>20,21</sup> silica surfaces,<sup>22,23</sup> and the mercury/water interface.<sup>24</sup> In spite of these claims, it has been argued that chemical binding accounts for most of the observations of charge inversion.<sup>16,25</sup> Subsequent works combining theory and experiment have shown examples in which solvation thermodynamics of the interface and the ions play an important role in charge inversion.<sup>18,26</sup> In ref 18, charge inversion due to the organic monovalent ion  $\text{Ph}_4\text{As}^+$  was observed, and the effect was attributed to the hydrophobic effect. In another recent work,<sup>26</sup> a combination of electrokinetic measurements and molecular dynamics simulations suggested that ion solvation properties were key to charge inversion in liposomes even with multivalent ions.

In spite of all the controversies, previous results seem to imply a link between solvation of ions and the hydrophobic or hydrophilic character of surfaces not only to specific ion effects but also to some examples of charge inversion. The plausibility of this link is precisely the problem we will discuss in this work, by combining experiments, simulations and theoretical calculations in both hydrophilic and hydrophobic colloids and organic and inorganic ions. The key finding of the work presented here is that interaction of monovalent ions with interfaces is dominated by solvation thermodynamics, that is, the chaotropic/kosmotropic character of ions and the hydrophobic/hydrophilic character of surfaces. In our experiments, charge inversion and ionic specific effects were simultaneously tuned according to the hydrophobic or hydrophilic nature of the interface. In our experiments reported here, the charge of both hydrophobic and hydrophilic cationic colloids is due to amine groups, so the observed effects cannot be attributed to pairing interactions with the charged groups of the colloids. A molecular insight on the observed results is provided with the help of computer simulations and multiscale calculations performed in a particular case. We argue that solvation thermodynamics is responsible for charge inversion with monovalent ions, which is accompanied by specific ion effects.

## II. METHODS

**A. Experimental Materials and Methods.** Our experimental studies consisted of electrophoretic measurements of dispersions of cationic hydrophobic and hydrophilic colloidal particles in solutions of different electrolytes. The cationic nature of both hydrophobic and hydrophilic colloids was due to the presence of amine groups at the

surface, which are positively charged under the conditions of our experiments ( $\text{pH} = 4$ ). In all electrolyte solutions, the cation was  $\text{Na}^+$ . We considered five different anions:  $\text{F}^-$ ,  $\text{Cl}^-$ ,  $\text{ClO}_4^-$ ,  $\text{SCN}^-$ , and  $\text{Ph}_4\text{B}^-$ .  $\text{ClO}_4^-$  is a highly symmetrical monovalent anion (radius about 2.83 Å) with a central chlorine atom at a high oxidized state (+7).  $\text{SCN}^-$  is a rod shaped anion which shares its negative charge approximately equally between sulfur and nitrogen.  $\text{Ph}_4\text{B}^-$  anion is a highly symmetrical, big anion (with a diameter about 0.9 nm) which consists of a central boron atom connected to four phenyl rings.

The hydrophobic colloids employed in this work were polystyrene latex particles obtained by emulsion polymerization method.<sup>27</sup> The surface of the particles showed amphoteric nature with an isoelectric point around 6 (see ref 7 and 27). The surface groups came from the initiator molecules used in the synthesis: methacrylic acid (carboxylic groups) and *N,N*-diethylaminoethyl methacrylate (amine groups) in a 1:1 molar relation. Consequently, the surface charge density ( $\sigma_0$ ) was not constant on pH. In all experiments considered here, we have  $\text{pH} = 4$ , so the particles were positively charged. The mean diameter, determined by transmission electron microscopy (TEM), was  $210 \pm 10$  nm, having a polydispersity index (PDI) very close to unity (1.010), which gives an idea about its size homogeneity.

The hydrophilic colloids employed in this work were core–shell lipid–chitosan nanocapsules. The diameters of these particles are around 200 nm and they have positive charge at  $\text{pH} = 4$ , provided by the glucosamine groups of chitosan which present a weak basic character. All the details concerning to particle synthesis and characterization can be found elsewhere.<sup>7,28</sup>

All the salts employed in this work were of analytical grade and purchased from different firms: Merck, Sigma, and Scharlau. Deionized Milli-Q water was used throughout. Nonbuffered solutions were obtained by adding HCl to water in the desired quantity to get  $\text{pH} 4$ .

The electrophoretic mobility measurements were performed with a Zetasizer Nano apparatus (Malvern Instruments) which allows one to measure electrophoretic mobility at high salt concentrations. Particles were diluted in the desired electrolyte solution, and mobility data was taken from the average of at least three measurements. The concentration of particles in the experiments was  $5 \times 10^{-9}$  particles/cm<sup>3</sup>. Experiments with two other concentrations also corresponding to diluted dispersions were performed to ensure that results do not depend on particle concentration as expected (data not shown).

**B. Estimation of Electrokinetic Charge from Mobility Measurements.** Once the electrophoretic mobility of colloids was measured, we estimated the electrokinetic charge density  $\sigma^{\text{ek}}$  which is a key quantity in the analysis of charge inversion experiments.<sup>16,29</sup> This quantity is interpreted as the amount of charge responsible for the observed electrokinetic motion and is obtained via the Grahame equation:

$$\sigma^{\text{ek}} = \sqrt{8\varepsilon_0\varepsilon_r c_0 RT} \sinh(F\zeta/2RT) \quad (1)$$

where the electrokinetic or  $\zeta$ -potential is related to the electrophoretic mobility  $\mu_E$  by

$$\zeta = (\eta/\varepsilon_0\varepsilon_r)\mu_E \quad (2)$$

Here,  $c_0$  is the bulk concentration of 1:1 electrolyte,  $\varepsilon_r$  and  $\eta$  are the dielectric constant and viscosity of water respectively,  $F$  is the Faraday constant, and the other symbols have their standard meaning. Let us recall that  $\sigma^{\text{ek}}$  accounts for both the charge coming from the colloid and any other sources such as adsorbed ions. In the case of indifferent electrolyte (no ionic adsorption), the electrokinetic charge obtained from eqs 1 and 2 is independent of electrolyte concentration and can be identified with the bare electrokinetic charge of the colloid, denoted by  $\sigma_0^{\text{ek}}$ . Adsorption or depletion of ions from the colloid is manifested by a strong dependence of  $\sigma^{\text{ek}}$  with concentration which is different for each electrolyte.

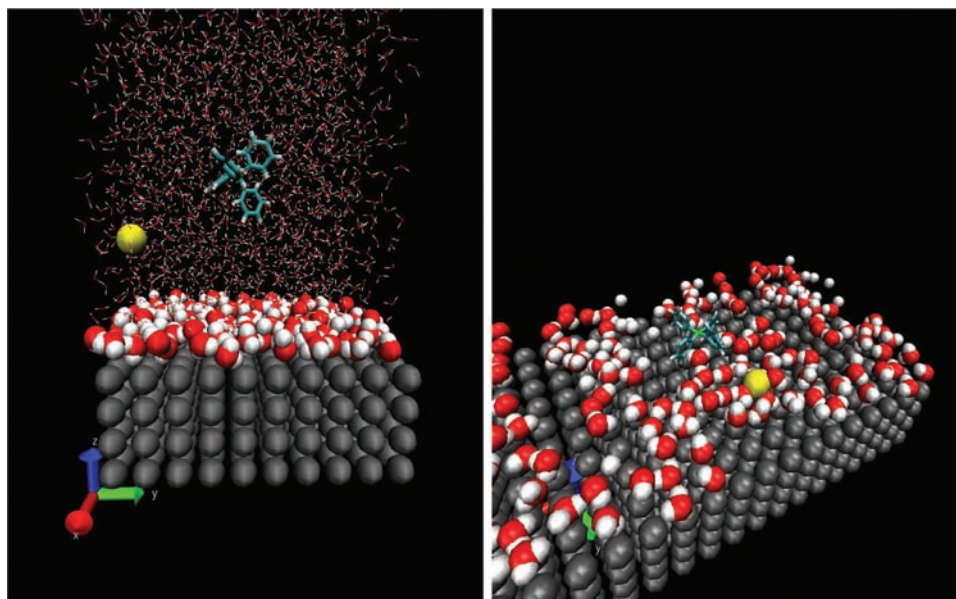


**Figure 1.** Snapshots from MD simulations.  $\text{Na}^+$  is shown as a yellow sphere, oxygen atoms are shown in red, hydrogen atoms are shown in white, carbon atoms are shown in cyan, and boron is shown in green. Atoms of the generic hydrophobic or hydrophilic surfaces are also shown in cyan. Left panel: front view of a simulation with hydrophilic surface (for simplicity, only water molecules in contact with the surface are shown in real size and all other molecules are shown as dots). Right panel: view of a simulation with a hydrophobic surface (for simplicity, only water molecules in contact with the surface are shown in real size and all other molecules are omitted).

### C. Methodology for the All-Atomic Simulations and Theoretical Calculations.

In order to obtain an atomistic view of the experiments described in the previous section, we have performed all-atomic molecular dynamics (MD) simulations. In order to characterize the water-mediated interaction of ions with the surface, our simulations are directed to the calculation of the potential of mean force of the ions with both hydrophobic and hydrophilic surfaces. We have considered only the case for which the experimental results showed larger and more interesting effects, which is the case of the  $\text{Ph}_4\text{B}^-\text{Na}^+$  electrolyte in contact with hydrophobic or hydrophilic surfaces. Also, a suitable force-field for this ion has been developed in previous work.<sup>30</sup> Note also that, in the case of simple inorganic anions, the choice of the force field is more complex due to the necessity of using polarizable force fields for some ions, so we prefer to avoid this issue and consider only simulations of  $\text{Ph}_4\text{B}^-\text{Na}^+$  electrolyte.

We employ a model and force field for the organic  $\text{Ph}_4\text{B}^-$  anion based on ab initio calculations.<sup>30</sup> The model employed for water is a modified TIP3P model following the standard specifications of the CHARMM27 force field. For the  $\text{Na}^+$  cation we employ also standard CHARMM27 parameters. The force field employed for both the hydrophobic and hydrophilic surfaces is based on the generic model proposed in previous studies of ionic specificity.<sup>31</sup> Given the complexity of the real surfaces present in our experiments, and the lack of sufficient structural information to build up a realistic model with atomistic detail, we believe that a generic model of this kind is the only feasible option. Other recent models, which include partial atomistic details (such as the models considered in refs 32–34) do not correspond to our experimental situation, and their generalization to our case seems to be far from trivial. In this generic model, the atomistic structure of the surface is identical in both the hydrophobic and hydrophilic case and is made of atoms modeled as Lennard–Jones spheres characterized by  $\sigma = 3.374 \text{ \AA}$  and  $\epsilon = 0.164 \text{ kcal/mol}$  for the hydrophobic surface and  $\epsilon = 2.084 \text{ kcal/mol}$  for the hydrophilic surface.

All simulations were performed using the NAMD2 program<sup>35</sup> running in parallel using 16 Itanium Monvale processors. The Newton equations of motion were solved with a time step of 2 fs, and electrostatic

interactions were updated with a 4 fs time step. All bonds between heavy atoms and hydrogen atoms were maintained rigid during all the simulations. The nonbonding Lennard–Jones interactions were cut off at a distance of 1.2 nm employing a switching function starting at 1.0 nm. The Ewald summation method was employed with a  $30 \times 30 \times 90$  grid size. A constant temperature of 298 K was maintained in all simulations using a Langevin thermostat with a relaxation constant of  $1 \text{ ps}^{-1}$ . In all our simulations, we employed periodic boundary conditions in all directions.

The MD simulations were performed as follows. First, we performed a 1 ns NPT run of a system containing a slab of pre-equilibrated water molecules, one  $\text{Ph}_4\text{B}^-$  anion and one  $\text{Na}^+$  cation (no surfaces). In these NPT simulations, the pressure (1 atm) was maintained using the Nosé–Hoover Langevin piston as implemented in NAMD with an oscillation period of 100 fs and a decay time of 50 fs. Then we put the resulting system in contact with a solid surface. We prepared two simulations, one with a hydrophobic surface and another with a hydrophilic surface. In these simulations, the solid surface was made of 400 atoms in a bcc structure with four equal layers of dimensions  $33.74 \text{ \AA} \times 33.74 \text{ \AA}$  each. In order to speed up simulations, the positions of all atoms of this solid are maintained fixed during the simulations, as in previous work.<sup>31</sup> In addition to this solid structure of hydrophobic or hydrophilic character, the simulation box contains one  $\text{Ph}_4\text{B}^-$  anion, one  $\text{Na}^+$  cation inside a water slab of  $\sim 5 \text{ nm}$  thickness (around  $\sim 1700$  water molecules). The solid is located at the bottom of the simulation box and a large vacuum is left at the top of the water slab. In each case, a NVT simulation run of 66 ns was performed. These long simulation times ensured proper equilibration of the system. Illustrative snapshots of these simulation runs are shown in Figure 1. Additionally we have performed MD simulations of water without ions in contact with the hydrophobic or hydrophilic surface. This was made as a reference simulation, in order to make possible to identify putative differences in the simulation results due to the presence of ions. These additional simulations are described in the Supporting Information.

It is interesting to note that in the simulation with a hydrophobic surface, the  $\text{Ph}_4\text{B}^-$  anion stays at the surface during almost all the

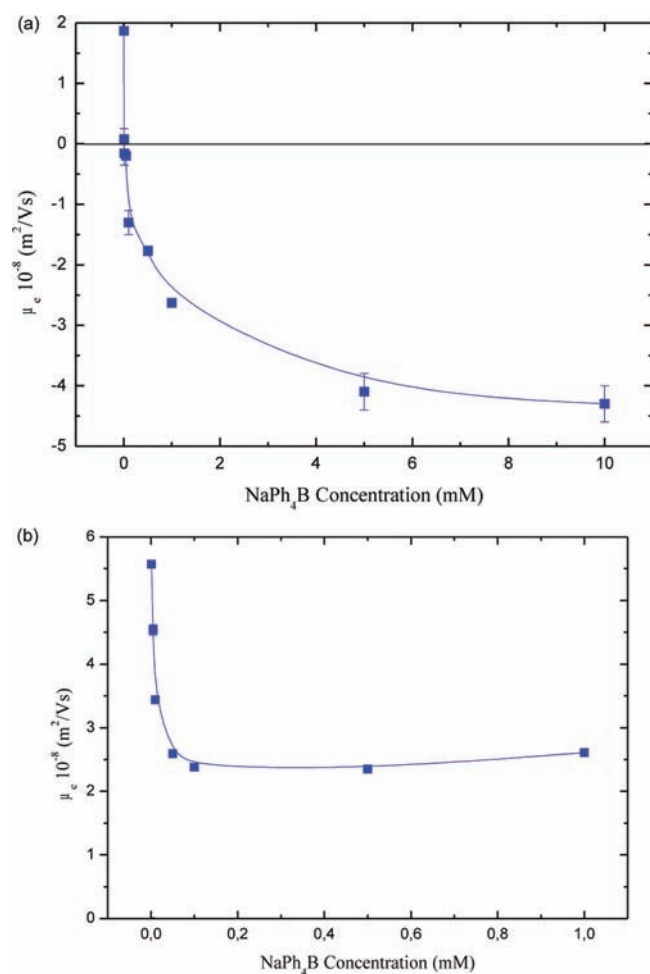


**Figure 2.** Measured electrophoretic mobility as a function of  $\text{Ph}_4\text{B}^- \text{Na}^+$  concentration for (a) hydrophobic and (b) hydrophilic colloids.

simulation. In the hydrophilic case, the  $\text{Ph}_4\text{B}^-$  is always found far from the surface. At this point, it was clear that further biased simulations were required to sample all possible separations between the ions and the surfaces. To this end, the final configurations of the NVT simulations were employed in further simulations designed to obtain the potential of mean force of the ions. These biased MD simulations were performed using the adaptive biasing force technique (MD-ABF) described in ref 36. This technique is implemented in the standard version 2.7 of NAMD. The force constant employed in the calculation was the default value of  $10 \text{ kcal/mol}/\text{\AA}^2$ . The reaction coordinate employed in the MD-ABF calculations was the distance between the center of the ion and the top of the solid surface. The potential of mean force of each ion was obtained with a  $0.2 \text{ \AA}$  resolution from contact to the surface up to  $3 \text{ nm}$  of separation. We performed a total of four different MD-ABF runs of  $5 \text{ ns}$  each in order to obtain the potential of mean force of  $\text{Ph}_4\text{B}^-$  and  $\text{Na}^+$  for the hydrophobic and the hydrophilic surface.

The results obtained in the previous MD-ABF calculations in presence of neutral hydrophilic or hydrophobic surfaces can be employed in order to predict the results in the case of charged hydrophobic or hydrophilic surfaces in contact with low concentrations of electrolyte. This can be done by employing a methodology proposed in previous works.<sup>34</sup> Let us here briefly summarize this approach. First of all, it is assumed that the density profile  $\rho_i(z)$  of each ion  $i$  is given by ( $\beta = 1/k_B T$ ):

$$\rho_i(z) = \rho_0 \exp(-\beta V_i^{\text{PMF}}(z) - \beta q_i \phi(z)) \quad (3)$$

where  $V_i^{\text{PMF}}(z)$  is the potential of mean force of ion  $i$  obtained from simulations performed with full atomistic detail (as those described previously in this subsection). In eq 3,  $\rho_0$  is the ionic density (number of ions per unit volume) at bulk, far from the surface, and the average electrostatic potential  $\phi(z)$  obeys the Poisson equation:

$$-\epsilon_0 \epsilon_r \frac{d^2}{dz^2} \phi(z) = \sum_i q_i \rho_i(z) \quad (4)$$

Equation 4 is subject to the boundary condition of bare charge density  $\sigma_0$  at the surface ( $z = 0$ ):

$$\epsilon_0 \epsilon_r \frac{d\phi}{dz} \Big|_{z=0} = -\sigma_0 \quad (5)$$

Note that, in comparing with electrokinetic experiments,  $\sigma_0$  should be taken as the bare electrokinetic charge, as determined from experiments with indifferent electrolyte. Once  $V_i^{\text{PMF}}(z)$  is obtained from MD simulations, the density profiles of the ions and the electrostatic potential are obtained by solving numerically eqs 3–5. In our case, the strong interactions encoded in the potential of mean force for the organic anions  $\text{Ph}_4\text{B}^-$  (as compared with the PMFs obtained in previous works on ionic specificity<sup>31,34</sup>) make technically difficult the numerical solution of eqs 3–5. For this reason, we have developed an advanced algorithm for the numerical solution which is explained in detail in the Supporting Information. The Fortran code developed for the numerical solution is also supplied to facilitate reproducibility of our results and use by other researchers.

### III. EXPERIMENTAL RESULTS

**A. Results for Organic Anion (Hydrophobic and Hydrophilic Surfaces).** In this section, we consider the effect of very diluted solutions of  $\text{Ph}_4\text{B}^- \text{Na}^+$  electrolyte on the electrokinetic behavior of hydrophilic and hydrophobic colloids. The electrophoretic mobility as a function of electrolyte concentration is shown in Figure 2. Our experimental results show that very low concentrations of  $\text{Ph}_4\text{B}^- \text{Na}^+$  have an impressive effect on the electrophoretic mobility of hydrophobic colloids (see Figure 2a). These positively charged colloids show inversion of electrophoretic mobility at extremely low concentrations. At  $5 \mu\text{M}$  concentration of  $\text{Ph}_4\text{B}^- \text{Na}^+$ , the measured electrophoretic mobility is  $\mu_E = 0.08 \times 10^{-8} \text{ m}^2/(\text{V s})$ , whereas at  $10 \mu\text{M}$  we have  $\mu_E = -0.16 \times 10^{-8} \text{ m}^2/(\text{V s})$ . As the concentration of organic anions increases, the magnitude of the inverted mobility increases dramatically. For comparison, let us note that at  $10 \text{ mM}$  concentration of  $\text{NaCl}$  (a nearly indifferent electrolyte), the mobility of the hydrophobic colloid is  $\mu_E = 3.5 \times 10^{-8} \text{ m}^2/(\text{V s})$ . At  $10 \text{ mM}$  concentration of  $\text{Ph}_4\text{B}^- \text{Na}^+$ , we obtain  $\mu_E = -4.5 \times 10^{-8} \text{ m}^2/(\text{V s})$ , which is larger in magnitude and opposite in sign. Therefore, we observe a large inversion of the electrophoretic mobility of the colloid at very low concentrations of organic anions. This inversion of mobility is only observed for hydrophobic colloids. In the case of hydrophilic colloids (see Figure 2b), the electrokinetic mobility decreases for low  $\text{Ph}_4\text{B}^- \text{Na}^+$  concentrations and then reaches a stable value.

In order to interpret the mobility results, it is helpful to compute the electrokinetic charge  $\sigma^{\text{ek}}$ . In Figure 3, we show the results for both hydrophobic and hydrophilic surfaces. For comparison, we also show the results obtained at very low concentrations of  $\text{NaCl}$ . It is remarkable that, at these low concentrations, there is little difference between the hydrophobic and hydrophilic cases with  $\text{NaCl}$  but there are striking differences in the case of  $\text{Ph}_4\text{B}^- \text{Na}^+$ . In the case of hydrophobic colloids, the

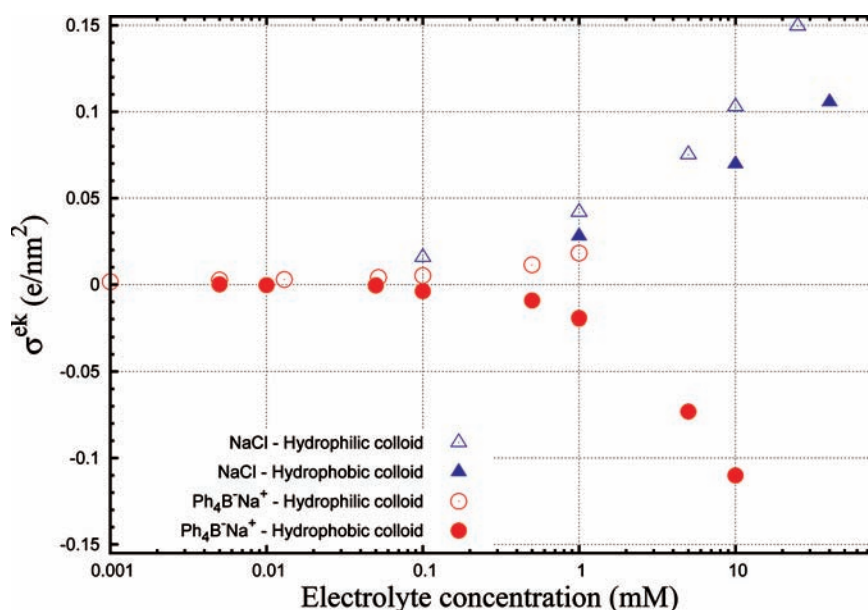


Figure 3. Electrokinetic charge computed from the mobility measurements reported in Figure 2 using eqs 1 and 2.

organic ions induce a negative electrokinetic charge larger in magnitude than the positive charge observed in presence of similar concentrations of NaCl. This charge inversion or charge reversal effect is of unprecedented magnitude. Inverted electrokinetic charges observed experimentally in previous works are only a few percent of the charge observed in presence of NaCl or KCl, so we can say that we observe here giant charge inversion. Also, the electrolyte concentrations typically required to obtain charge reversal are orders of magnitude larger than those observed here. In the case of a hydrophilic colloid, charge inversion is not observed. We obtain an increase of the electrokinetic charge as the concentration of  $\text{Ph}_4\text{B}^-\text{Na}^+$  increases, but the observed charge is of smaller magnitude than that observed in presence of NaCl.

At this point, it is important to emphasize some conclusions which can be extracted from these experimental results. First of all, it is clear that ionic correlations (due to ionic size and charge<sup>19,20</sup>) are not responsible here for charge inversion, in spite of being  $\text{Ph}_4\text{B}^-$  a large anion. Second, the strong interaction observed here between the anion and the cationic colloids cannot be attributed to the pairing between the anions and the positively charged surface groups because both colloids present weakly hydrated amino groups but the results are quite different depending on the hydrophobic or hydrophilic nature of the surface. Hence, the pairing mechanism proposed by Collins for ionic specificity<sup>4,9</sup> does not occur in our experiments. In our experiments, the overall hydrophobic or hydrophilic nature of the colloid surface is crucial. Now, our next step will be to investigate whether the same trends are observed (or not) with inorganic anions. The molecular origin of these observed effects will be left to the next section.

**B. Results for Inorganic Ions (Hydrophobic and Hydrophilic Surfaces).** In Figure 4a, we show experimental results for different inorganic salts and hydrophobic colloids. We have considered two poorly solvated inorganic anions,  $\text{ClO}_4^-$  and  $\text{SCN}^-$ , which have very low hydration numbers and favorable free energy of transfer from water to organic solvents. For comparison, we also consider  $\text{F}^-$ , which is a highly solvated

ion with a strong affinity for hydrophilic surfaces,<sup>7,8,34</sup> and it is known to be depleted from hydrophobic surfaces and also from the air–water interface.<sup>11</sup> We also consider  $\text{Cl}^-$ , which has an intermediate (nearly indifferent) character. As shown in Figure 4a, mobility curves follow a clear ordering, depending on the aforementioned nature of the anion. In fact, our results show that the mobility of hydrophobic latex colloid with different inorganic ions follows direct Hofmeister series, in agreement with previous results in hydrophobic systems.<sup>7,8</sup> We observe that, under the same electrolyte concentrations, colloids have higher mobilities in the presence of better hydrated anions than in the presence of poorly solvated ions.  $\text{F}^-$  is repelled by the colloid surface, and  $\text{ClO}_4^-$  and  $\text{SCN}^-$  are strongly attracted to the colloid surface, even inducing reversal of the electrophoretic mobility and hence charge inversion. As expected,  $\text{Cl}^-$  shows an intermediate character.

To the best of our knowledge, this is the first experimental demonstration of charge inversion by inorganic monovalent ions in latex colloids. In the case of latex colloids, charge inversion is typically observed by employing multivalent ions, an observation that has fueled electrostatic interpretations for the driving force of charge inversion phenomena.<sup>14,15</sup> Therefore, the charge inversion observed with  $\text{ClO}_4^-$  and  $\text{SCN}^-$  deserves further consideration. First of all, it is clear that the hydrophobic nature of the colloid is essential to observe charge inversion. Our measurements made in the case of hydrophilic colloids (Figure 4b) show that charge inversion is absent in this case and ionic specificity disappears. The striking differences between the hydrophobic and hydrophilic case are even more clear in Figure 5. In this figure, we show the electrokinetic charge for both the hydrophilic and hydrophobic case with  $\text{Cl}^-$ ,  $\text{ClO}_4^-$ , and  $\text{SCN}^-$ . In the hydrophilic case, all three ions give almost identical results. In the hydrophobic case,  $\text{Cl}^-$  gives always a positive electrokinetic charge (around  $0.1 \text{ e/nm}^2$ ), whereas  $\text{ClO}_4^-$  and  $\text{SCN}^-$  give substantial charge reversal (up to  $-0.15 \text{ e/nm}^2$  for the highest concentrations). The results obtained here for inorganic ions are of course in line with our results presented in the previous subsection for organic ions. Hydrophobicity of the surface is

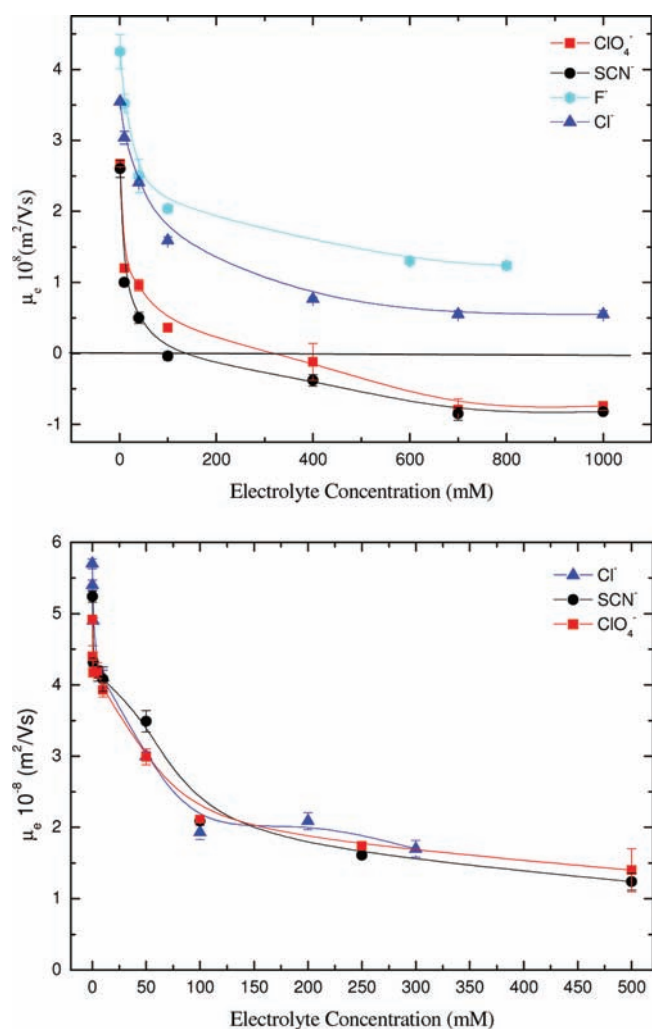


**Figure 4.** Measured electrophoretic mobility of colloids as a function of concentration for different inorganic salts. Top: hydrophobic colloids. Bottom: hydrophilic colloids.

therefore an essential ingredient to obtain charge inversion which is obtained with poorly solvated inorganic or organic ions.

#### IV. THEORETICAL RESULTS AND INTERPRETATION OF EXPERIMENTAL RESULTS

**A. Simulation and Multiscaling Results.** In order to obtain a molecular insight on the obtained results, we have performed the simulations and theoretical analysis described in the Methods section.

First, let us comment on the behavior of water near the generic model of hydrophobic and hydrophilic surfaces considered in our simulations. As shown in Figure 6, the density profile of water depends strongly on the hydrophobic or hydrophilic nature of the surface. The results are in quantitative agreement with previous simulation results of water near different kinds of hydrophobic and hydrophilic surfaces.<sup>31,33</sup> Near the hydrophilic surface, water shows a strong structuration, with strong peaks and oscillations in the density which decay away after distances about 0.7 nm. As in previous work, a similar decay is observed in the profiles of other water properties such as orientation of water molecules or average number of hydrogen bonds (see the

Supporting Information). As expected, water shows much less structure (and also shows a slight depletion) near the hydrophobic surface. It is interesting to note that the size of this small depletion region is very similar to that found in ref 33 for different hydrophobic surfaces but smaller than the large 3 Å dry gap found in the simulations of ref 32.

Now, we would like to study the interaction of hydrophobic and hydrophilic surfaces with  $\text{Ph}_4\text{B}^- \text{Na}^+$  electrolyte. To this end, we follow a two-step multiscaling approach, as described in the Methods section (see also previous works such as ref 34). First, we perform molecular dynamics simulations in order to characterize the water mediated interaction of the electrolyte with neutral hydrophobic and hydrophilic surfaces, obtaining the free energy profile (potential of mean force). Second, we use the simulation results to obtain numerically the ionic profiles for charged hydrophobic and hydrophilic surfaces at given electrolyte concentration.

Our results show that the interaction of the  $\text{Ph}_4\text{B}^-$  ion with the surface is strongly affected by the hydrophobic or hydrophilic character of the surface. In Figure 7, we show our results for the potential of mean force (PMF) for the  $\text{Ph}_4\text{B}^-$  ion, which characterizes the interaction of this anion with neutral interfaces. We found a repulsive barrier for the  $\text{Ph}_4\text{B}^-$  anion in the case of a hydrophilic surface and a clear adsorption minimum in the case of a hydrophobic surface (see Figure 7). Interestingly, we found that the range of the potential of mean force is similar to the range of water structure induced from the surface (compare Figures 6 and 7). Also, the depth of the adsorption minimum shown in Figure 7 has a thermodynamical interpretation in terms of solvation free energy, which will be discussed in the next subsection.

The same calculation for the potential of mean force has been made with the  $\text{Na}^+$  ion. The results (not shown) are equivalent to those obtained in previous work (see for example refs 31 and 34). As demonstrated in these previous calculations,  $\text{Na}^+$  has a slight preference for the hydrophilic surface. In any case, the involved free energy (of the order of a  $k_B T$ ) is very small as compared to that reported here for the  $\text{Ph}_4\text{B}^-$  anion, so in the following we will neglect this specific interaction of  $\text{Na}^+$  with the surface.

Now, let us discuss our results in the case of charged hydrophobic or hydrophilic surfaces. In Figure 8 we show the predictions of eqs 3–5 for hydrophobic and hydrophilic surfaces, employing the potential of mean force shown in Figure 7 for the  $\text{Ph}_4\text{B}^-$  anion. In both cases, the surfaces have a charge density  $\sigma_0 = 0.12 \text{ e/nm}^2$  ( $1.9 \mu\text{C/cm}^2$ ), typical of representative real colloids (see our previous experimental results and also characterization data in refs 7 and 28). As a representative example, we consider a bulk concentration of 0.1 mM of  $\text{Ph}_4\text{B}^- \text{Na}^+$ , corresponding to a Debye length  $\lambda_B \approx 3 \text{ nm}$ . As should be expected from our previous discussion, the distribution of ions is affected in a dramatic way by the hydrophobic or hydrophilic character of the surfaces.

In the case of the hydrophobic surface, there is an impressive peak of concentration (4 orders of magnitude larger than bulk concentration) of anions near the surface in a very narrow region ( $\sim 0.4 \text{ nm}$ ). We interpret this result as evidence for the formation of a Stern layer in the sense employed in traditional colloidal science. In our calculations, the driving force for the formation of this compact layer is the hydrophobic effect. Near this Stern layer, there is a small depletion of  $\text{Ph}_4\text{B}^-$  anions and a similar excess of  $\text{Na}^+$  within a typical distance of the order of the Debye length. In this diffuse layer, the surface behaves as a negatively charged surface, and hence, we observe charge inversion due to the

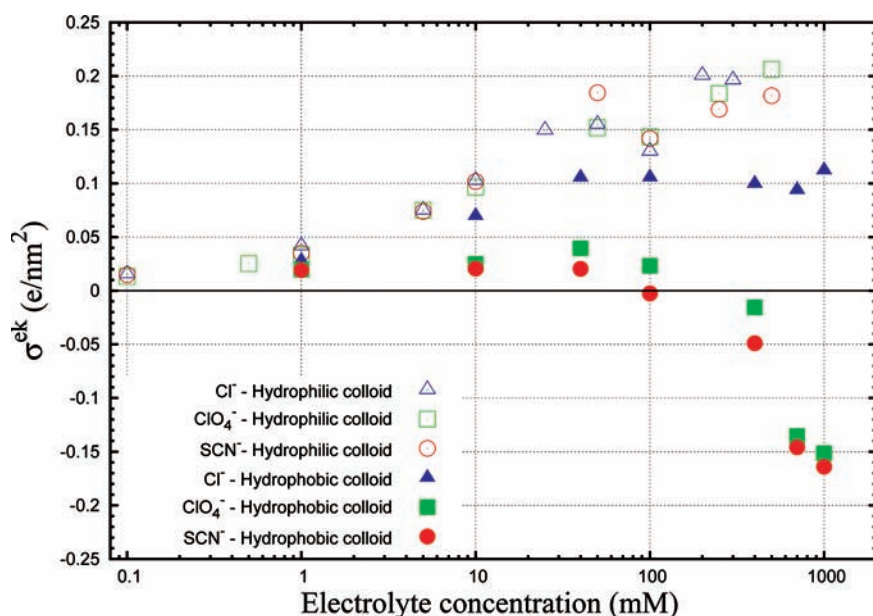


Figure 5. Electrokinetic charge computed from mobility measurements reported in Figure 4 using eqs 1 and 2.

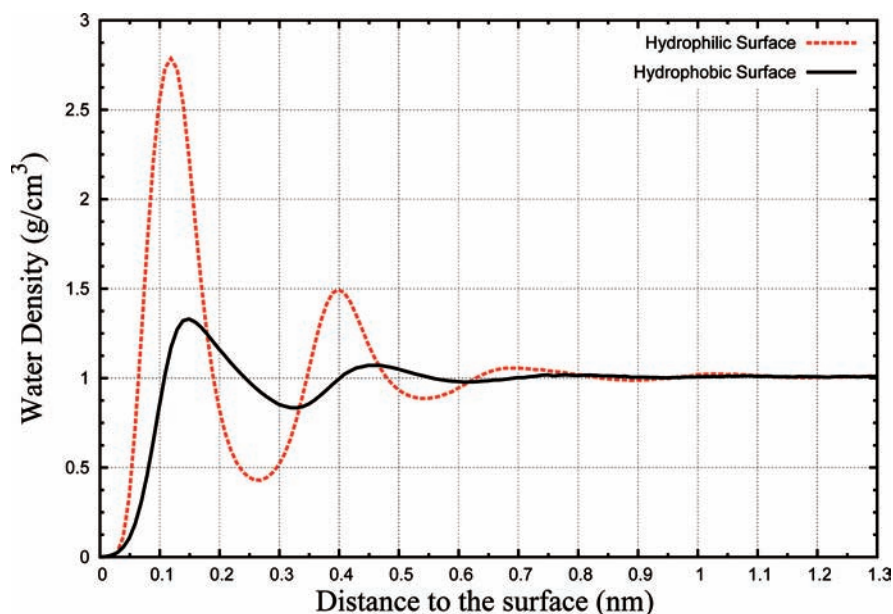
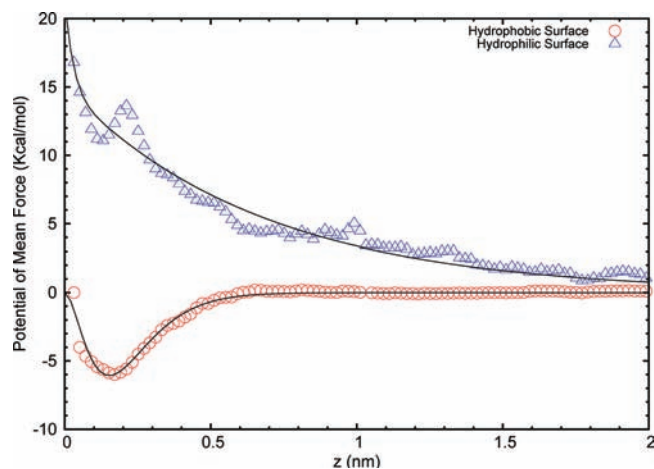


Figure 6. Density of water as a function of distance from surfaces of hydrophobic (solid lines) or hydrophilic (dashed lines) character, as obtained from MD simulations (distance is measured from top of surface atoms).

hydrophobic effect. In the case of the hydrophilic surface, we observe a completely different phenomenology. First of all, there is a depletion of  $\text{Ph}_4\text{B}^-$  anions in a layer of substantial thickness (about 2 nm). Also, the concentration of  $\text{Na}^+$  is substantially reduced near the surface due to the low concentration of anions which do not significantly screen the cationic charge of the surface at these distances. These results obtained for the hydrophilic surface cannot be interpreted with the help of classical concepts of colloidal science (such as the Stern layer and the diffuse layer) and require more sophisticated modeling.

The calculations leading to Figure 8a can be performed systematically for different values of the bare charge of the

colloid,  $\sigma_0$ , and different electrolyte concentrations. In this way, it is possible to determine the minimum concentration  $c_1$  of  $\text{Ph}_4\text{B}^- \text{Na}^+$  required to induce charge inversion for a hydrophobic surface as a function of  $\sigma_0$  (see ref 37 for details of the procedure). Our results, shown in Figure 9, predict that the charge inversion concentrations are extremely small, less than 0.5 mM for realistic values of  $\sigma_0$ , in agreement with our experimental observations. Another relevant result of Figure 9 is that the charge inversion concentration  $c_1$  depends linearly on the charge density  $\sigma_0$  of the surface. This behavior has interesting implications which will be discussed in the next subsection.



**Figure 7.** Potential of mean force  $V^{\text{PMF}}(z)$  for the  $\text{Ph}_4\text{B}^-$  anion as obtained in MD-ABF simulations ( $z = 0$  corresponds to the distance of closest approach between the anion and the surface). Circles correspond to simulations with a hydrophobic surface and triangles to simulations with a hydrophilic surface. The solid lines are fits to the simulation results in order to employ the  $V^{\text{PMF}}(z)$  function in further calculations.

**B. A Minimal Thermodynamic Model for Charge Inversion.** In previous works,<sup>18,38</sup> a simple relation between the charge inversion concentration  $c_1$  and the adsorption free energy per ion  $\Delta\mu_0$  has been proposed:

$$c_1 = \frac{\sigma_0}{qH} \exp(\Delta\mu_0/k_B T) \quad (6)$$

where  $q$  is the charge of the counterion and  $H$  can be interpreted as the thickness of the layer of adsorbed ions or the typical distance in which the interaction responsible for counterion adsorption is significant. Equation 6 is derived in refs 18 and 38 as a consequence of imposing thermodynamic equilibrium between the layer of adsorbed counterions and the bulk electrolyte. Equation 6 can be interpreted as a minimal thermodynamical model describing charge inversion. This expression has been employed in many previous works to interpret experimental results (see, for example, refs 18 and 38), but its validity is far from obvious, due to the crude assumptions employed in its derivation. In fact, the linear dependence of  $c_1$  with  $\sigma_0$  predicted by eq 6 has not been tested systematically in previous simulation and experimental works. This is due to the large amount of experiments or simulations needed to test this relation, since it requires extensive investigation of the effect of concentration in different systems with different  $\sigma_0$ . To the best of our knowledge, the result summarized in Figure 9 provides the first compelling evidence for the linear relation predicted by eq 6.

Now, we evaluate the free energy  $\Delta\mu_0$  appearing in eq 6 from a linear fit of the multiscaling calculation results (dots in Figure 9). From Figure 7, we see that the attraction of  $\text{Ph}_4\text{B}^-$  anions to the hydrophobic surface has a typical decay length of  $H \approx 0.5$  nm, which is of the order of the radius of the anion. Using this value for  $H$ , the fit of Figure 9 with eq 6 gives  $\Delta\mu_0 \approx -8.5k_B T$ . This result is not merely the result of a fit, but it has a clear thermodynamic interpretation: it is about half the free energy gain estimated for the transfer of this anion from water to organic solvents.<sup>39</sup> In fact, it is to be expected that, when adsorbing at a planar surface, the organic anion perturbs around half the amount of water as compared to being in bulk water replacing it

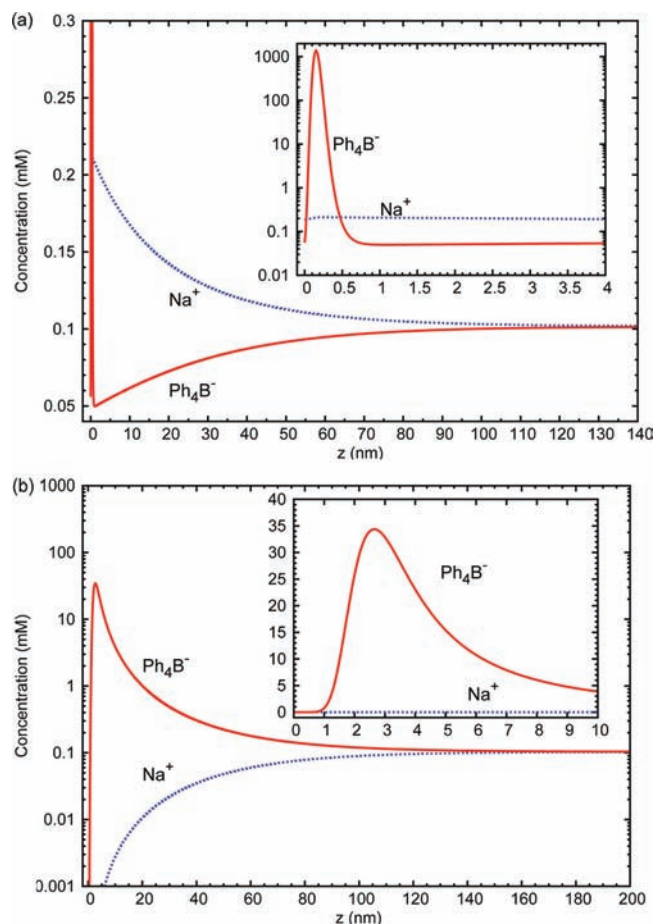


**Figure 8.** Concentration profiles calculated using the multiscaling approach for surfaces with charge density  $\sigma_0 = 0.12$  e/nm<sup>2</sup>. (a) Hydrophobic surface in contact with 0.1 mM  $\text{Ph}_4\text{B}^- \text{Na}^+$ . The inset shows a magnification of the region close to the surface with a strong peak of  $\text{Ph}_4\text{B}^-$  concentration. (b) Hydrophilic surface in contact with 0.1 mM  $\text{Ph}_4\text{B}^- \text{Na}^+$ . The inset shows a magnification of the first 10 nm from the surface. Note that we found charge reversal in (a) but not in (b).

with the interaction with the hydrophobic surface, so it gains about half of its water to organic solvent transfer free energy.

It is also worth noting that the obtained free energy gain  $\Delta\mu_0$  is larger than that obtained from charge inversion experiments of anionic colloids in presence of  $\text{Ph}_4\text{As}^+$  ( $-6k_B T$  in that case; see ref 18). This latter ion is strikingly similar to the  $\text{Ph}_4\text{B}^-$  ion considered here in the sense that both have essentially the same size and shape and the same organic groups which are responsible for the interaction with surfaces and water, with the cationic versus anionic character being the only significant difference. It is also known from experiments<sup>39</sup> and simulations<sup>30</sup> that the transfer of  $\text{Ph}_4\text{B}^-$  from water to organic solvents is more favorable than that of  $\text{Ph}_4\text{As}^+$ . Overall, all this evidence reinforces the view that solvation effects and ionic specific effects are more pronounced in anions than in cations similar in size, charge, and chemical composition. Now we see that also the same rule applies to charge inversion.

As in the previous case of organic ions, we can also understand the charge inversion obtained for  $\text{SCN}^-$  and  $\text{ClO}_4^-$  using the simple thermodynamical model given by eq 6. The evaluation of this relation requires the knowledge of (1) the size of the ion (which gives the parameter  $H$ ) and (2) an estimation of the



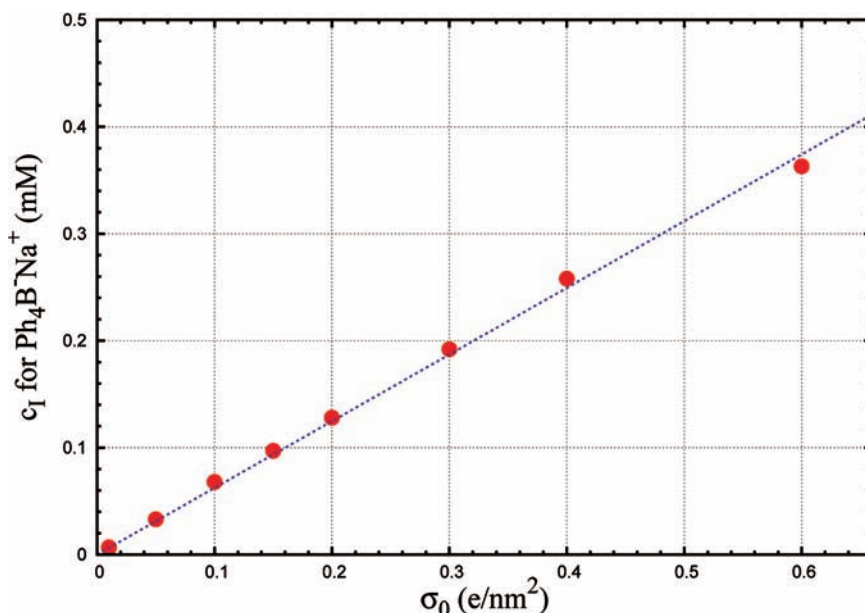


**Figure 9.** Minimum concentration of  $\text{Ph}_4\text{B}^- \text{Na}^+$  required to induce charge inversion in hydrophobic surfaces with charge density  $\sigma_0$ . Dots: Multiscale calculation (see text). Solid line, prediction of the simple model (eq 6) with  $\Delta\mu^{(0)} \approx -8.5k_B T$  and  $H \approx 0.5$  nm.

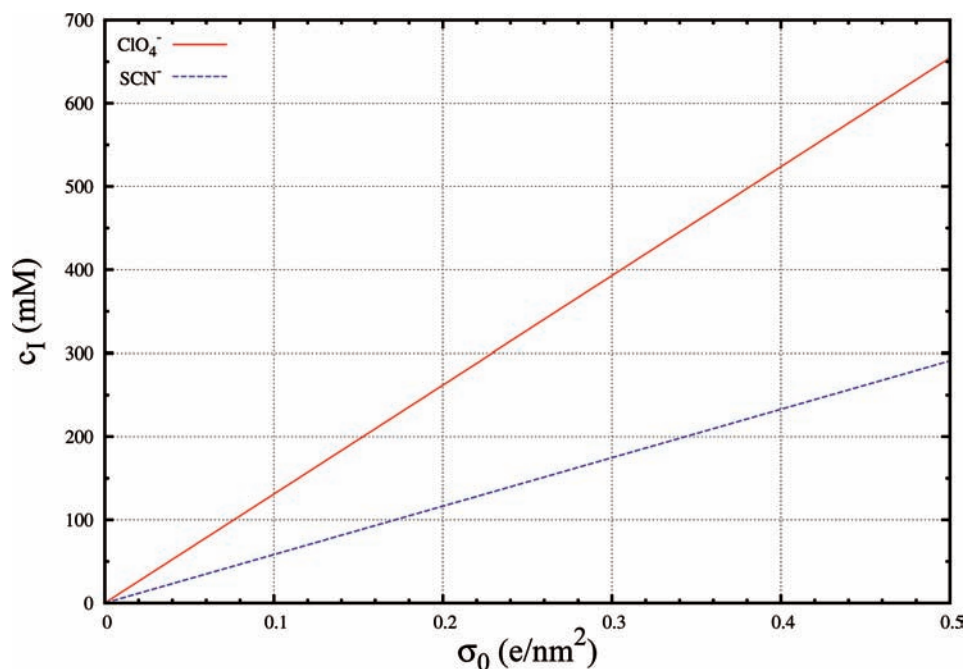


**Figure 10.** Minimum concentration of chaotropic anions ( $\text{SCN}^-$  or  $\text{ClO}_4^-$ ) required to induce charge inversion in hydrophobic surfaces with bare charge density  $\sigma_0$ , according to eq 6 (see main text for the values of the parameters  $\Delta\mu^{(0)}$  and  $H$  for these ions).

parameter  $\Delta\mu_0$  from independent, thermodynamical data, involving adsorption at interfaces under well-defined conditions and or transfer from water to organic solvents. In Figure 10, we show the results for reasonable choices of these parameters (discussed below). It is worth noting the striking difference between organic and inorganic ions (compare Figure 9 with Figure 10), which differ in several orders of magnitude in the electrolyte concentration needed to induce charge inversion.

Let us now discuss the parameters employed for the  $\text{SCN}^-$  ion in the calculation shown in Figure 10. This ion has the shape of a

cylinder, with radius 1.42 Å and length 4.77 Å. In previous experimental and theoretical works, it has been shown that this ion tends to adsorb flat at interfaces and surfaces, so we will take  $H \approx 1.42$  Å. Measurements of adsorption of  $\text{SCN}^-$  at the water–air interface<sup>40</sup> yield a Gibbs free energy of adsorption of  $-1.80$  kcal/mol. This value is approximately half the value of the typical free energy of transfer between water and different organic solvents,<sup>39</sup> so we will take  $\Delta\mu_0 \approx -1.8$  kcal/mol  $\approx -3k_B T$ . Using these values in eq 6, we obtain the relation between charge inversion concentration and colloid charge  $\sigma_0$  shown in

Figure 10. In the case of our experiments with hydrophobic colloids, the results with NaCl suggest a value of  $\sigma_0 \approx 0.11 \text{ e}/\text{nm}^2$ . For this value of  $\sigma_0$ , eq 6 predicts charge inversion at 64 mM concentration of  $\text{SCN}^-$  (see also Figure 10), in excellent agreement with our experimental results (see Figures 4 and 5).

In the case of  $\text{ClO}_4^-$ , we can approximate this ion as a sphere of radius 2.83 Å as in previous studies.<sup>11</sup> For the parameter  $\Delta\mu^0$ , we have not found experimental results as clear as the adsorption isotherms obtained in ref 40 for  $\text{SCN}^-$ . However, we see that, in general, transfer free energies of  $\text{ClO}_4^-$  between water and different solvents listed in the review of Marcus<sup>39</sup> are about half of the values observed for  $\text{SCN}^-$ . Hence, we take as an estimate  $\Delta\mu_0 \approx -1.5k_B T$ . Using these values in eq 6, we obtain the relation between charge inversion concentration and colloid charge  $\sigma_0$  shown in Figure 10. Again, we can compare with our experimental results, which correspond to a electrokinetic bare charge about  $\sigma_0 \approx 0.11 \text{ e}/\text{nm}^2$ . For this value of  $\sigma_0$ , eq 6 predicts charge inversion at 144 mM concentration of  $\text{ClO}_4^-$  (see also Figure 10, in reasonable agreement with our experimental results (see Figure 4b or 5)).

## V. CONCLUSIONS

In this work, we have discussed experimentally and theoretically the interaction of monovalent organic and inorganic anions with hydrophobic and hydrophilic colloids. In the case of hydrophobic colloids, our experimental results (see Figures 4 and 5) show that charge inversion is induced by poorly solvated inorganic monovalent ions ( $\text{ClO}_4^-$  and  $\text{SCN}^-$ ) but it is not induced by kosmotropic anions. The organic anion  $\text{Ph}_4\text{B}^-$  also shows charge inversion, which appears at extremely low electrolyte concentrations (a few micromolar) and reaches a large magnitude at millimolar concentrations (see Figures 2 and 3). The charge inversion effect disappears for both organic and inorganic ions when turning to hydrophilic colloids, demonstrating the decisive role played by the nature of the surface in the charge inversion problem.

It is worth noting that the solvation properties of the surface are typically neglected in theoretical and simulation studies of charge inversion.<sup>14,15,19–21,23</sup> Our results point out to the necessity of including a description of the hydration properties of both ions and surfaces in theoretical studies of charge inversion. Our results are also in line with the interpretation provided in ref 18 for the observed charge inversion in colloids with the organic cation  $\text{Ph}_4\text{As}^+$ , the results in ref 26 for charge inversion in anionic phospholipid liposomes with  $\text{La}^{3+}$ , and recent theoretical work on colloidal stability.<sup>12</sup>

In order to provide an atomistic understanding of our observations, we have performed molecular dynamics (MD) simulations with full atomic detail for the case of the  $\text{Ph}_4\text{B}^-$  ion interacting with both hydrophilic and hydrophobic surfaces. Also, employing a multiscale approach, we can extend our simulation results to a variety of situations with different electrolyte concentrations and surface charge. Our results show explicitly how the large adsorption free energies found for hydrophobic colloids are transformed into large repulsive barriers for hydrophilic colloids. A thermodynamical analysis of our multiscale results confirm that solvation free energy (and hence the hydrophobic effect) is the driving force for the buildup of a Stern layer of adsorbed ions and charge inversion in hydrophobic

colloids and it is also the mechanism preventing charge inversion in hydrophilic colloids.

It is also interesting to comment on the possible relation of our results and the law of matching affinities proposed by Collins<sup>4,6,9</sup> for the rationalization of specific ionic effects (particularly in biology). We have shown that the particular mechanism proposed in these works (pairing between charged entities of opposite charge and matching solvation) cannot explain our experiments, since both hydrophobic and hydrophilic colloids have their cationic charge from the same chemical groups but they interact differently with anions. But, in principle, it is conceivable that the mechanism for ionic specificity operating in proteins and colloids could be different. However, it is also true that our results can be understood as following a more general statement of this law of matching affinities, in which association results from the matching solvation free energies of ions and the surface of the colloids (not the particular charged groups present on the surface). In any case, we can say that our experimental and simulation results show that the interaction of monovalent ions with interfaces is dominated by solvation thermodynamics, that is, the chaotropic/kosmotropic character of ions and the hydrophobic/hydrophilic character of surfaces, in agreement with this concept.

## ■ ASSOCIATED CONTENT

**S Supporting Information.** Document with the detailed description of simulation methodology and numerical calculations. Fortran program for the numerical solutions of eqs 3–5. This material is available free of charge via the Internet at <http://pubs.acs.org>

## ■ AUTHOR INFORMATION

### Corresponding Authors

[jfaraudo@icmab.es](mailto:jfaraudo@icmab.es); [dbastos@ugr.es](mailto:dbastos@ugr.es)

## ■ ACKNOWLEDGMENT

This work is supported by the Spanish Government (Grants MAT2009-13155-C04-02, FIS2009-13370-C02-02, and CONSOLIDER-NANOSELECT-CSD2007-00041), Junta de Andalucía (Grants P07-FQM-2496 and CTS-6270), and Generalitat de Catalunya (2009SGR164). C.C. is supported by a JAE doc contract (CSIC). Supercomputing resources were provided by the CESGA Supercomputing Center, Spain. We thank Main Okdeh and Paola Sánchez for their help in some experiments.

## ■ REFERENCES

- (1) Evans, D. F.; Wennerström, H. *The Colloidal Domain*, 2nd ed.; VCH: New York, 1999.
- (2) Kunz, W. *Curr. Opin. Colloid Interface Sci.* **2010**, *15*, 34.
- (3) Kunz, W.; Neueder, R., Eds. *Specific Ion Effects*, 1st ed.; World Scientific Co. Pte. Ltd.: Singapore, 2009.
- (4) Collins, K. D.; Neilson, G.; Enderby, J. *Biophys. Chem.* **2007**, *128*, 95.
- (5) Zangi, R. *J. Phys. Chem. B* **2010**, *114*, 643.
- (6) Collins, K. D. *Biophys. J.* **1997**, *72*, 65.
- (7) López-León, T.; Santander-Ortega, M. J.; Ortega-Vinuesa, J. L.; Bastos-González, D. *J. Phys. Chem. C* **2008**, *112*, 16060.
- (8) Peula-García, J. M.; Luis Ortega-Vinuesa, J.; Bastos-González, D. *J. Phys. Chem. C* **2010**, *114*, 11133.
- (9) Collins, K. D. *Methods* **2004**, *34*, 300.

- (10) Levin, Y.; dos Santos, A. P.; Diehl, A. *Phys. Rev. Lett.* **2009**, *103*, 257802.
- (11) dos Santos, A. P.; Diehl, A.; Levin, Y. *Langmuir* **2010**, *26*, 10778.
- (12) dos Santos, A. P.; Levin, Y. *Phys. Rev. Lett.* **2011**, *106*, 167801.
- (13) Caleman, C.; Hub, J.; van Maaren, P.; van der Spoel, D. *Proc. Natl. Acad. Sci.* **2011**, *108*, 6838.
- (14) Grosberg, A.; Nguyen, T.; Shklovskii, B. *Rev. Mod. Phys.* **2002**, *74*, 329.
- (15) Levin, Y. *Rep. Prog. Phys.* **2002**, *65*, 1577.
- (16) Lyklema, J. *Colloids Surf., A* **2006**, *291*, 3.
- (17) Faraudo, J.; Travesset, A. *J. Phys. Chem. C* **2007**, *111*, 987.
- (18) Martín-Molina, A.; Calero, C.; Faraudo, J.; Quesada-Pérez, M.; Travesset, A.; Hidalgo-Álvarez, R. *Soft Matter* **2009**, *5*, 1350.
- (19) Guerrero-García, G.; González-Tovar, E.; de la Cruz, M. O. *Soft Matter* **2010**, *6*, 2056.
- (20) Quesada-Pérez, M.; González-Tovar, E.; Martín-Molina, A.; Lozada-Cassou, M.; Hidalgo-Álvarez, R. *ChemPhysChem* **2003**, *4*, 235.
- (21) Martín-Molina, A.; Maroto-Centeno, J.; Hidalgo-Álvarez, R.; Quesada-Pérez, M. *Colloids Surf., A* **2008**, *319*, 103.
- (22) van der Heyden, F.; Stein, D.; Besteman, K.; Lemay, S.; Dekker, C. *Phys. Rev. Lett.* **2006**, *96*, 224502.
- (23) Labbez, C.; Jonsson, B.; Skarba, M.; Borkovec, M. *Langmuir* **2009**, *25*, 7209.
- (24) Wernersson, E.; Kjellander, R.; Lyklema, J. *J. Phys. Chem. C* **2010**, *114*, 1849.
- (25) Lyklema, J. *Adv. Colloid Interface Sci.* **2009**, *147–48*, 205.
- (26) Martín-Molina, A.; Rodríguez-Beas, C.; Faraudo, J. *Phys. Rev. Lett.* **2010**, *104*, 168103.
- (27) Valle-Delgado, J.; Molina-Bolivar, J. A.; Galisteo-González, F.; Gálvez-Ruiz, M. J. *Colloid Polym. Sci.* **2003**, *281*, 708.
- (28) Santander-Ortega, M.; Lozano-López, M.; Bastos-González, D.; Peula-García, J.; Ortega-Vinuesa, J. L. *Colloid Polym. Sci.* **2010**, *288*, 159.
- (29) Lyklema, J. *Colloids Surf., A* **2011**, *376*, 2.
- (30) Schurhammer, R.; Wipff, G. *J. Phys. Chem. A* **2000**, *104*, 11159.
- (31) Huang, D. M.; Cottin-Bizonne, C.; Ybert, C.; Bocquet, L. *Langmuir* **2008**, *24*, 1442.
- (32) Janeek, J.; Netz, R. *Langmuir* **2007**, *23*, 8417.
- (33) Godawat, R.; Jamadagni, S.; Garde, S. *Proc. Natl. Acad. Sci. U.S.A.* **2009**, *106*, 15119.
- (34) Schwierz, N.; Horinek, D.; Netz, R. *Langmuir* **2010**, *26*, 7370.
- (35) Phillips, J.; et al. *J. Comput. Chem.* **2005**, *26*, 1781.
- (36) Hénin, J.; Fiorin, J.; Chipot, C.; Klein, M. *J. Chem. Theory Comput.* **2010**, *6*, 35.
- (37) Calero, C.; Faraudo, J. *Phys. Rev. E* **2009**, *80*, 042601.
- (38) Besteman, K.; Zevenbergen, M.; Lemay, S. *Phys. Rev. E* **2005**, *72*, 061501.
- (39) Marcus, Y. *Chem. Rev.* **2007**, *107*, 3880.
- (40) Petersen, P.; Saykally, R.; Mucha, M.; Jungwirth, P. *J. Phys. Chem. B* **2005**, *109*, 10915.